AGRICULTURAL WATER MANAGEMENT

Type of paper: original research paper (regular paper)

Title: Effects of saline reclaimed waters and deficit irrigation on *Citrus* physiology assessed by UAV remote sensing.

Authors names and addresses:

Cristina **Romero-Trigueros***[1], Pedro A. **Nortes**[1], Juan J. **Alarcón**[1]**,** Johannes E. **Hunink**[2], Margarita **Parra**[1], Sergio **Contreras**[2], Peter **Droogers**[2], Emilio **Nicolás**[1]**.**

[1]Departamento de Riego, Centro de Edafología y Biología Aplicada del Segura, CSIC, P.O. Box 164, 30100, Espinardo (Murcia), Spain

[2]Future Water, Paseo Alfonso XIII, 48, 30203, Cartagena, Spain.

Corresponding author: Cristina Romero-Trigueros

Departamento de Riego

Centro de Edafología y Biología Aplicada del Segura, CEBAS-CSIC.

Campus Espinardo P.O. Box 164, 30100, Espinardo (Murcia), Spain

Phone: +34 968 396200 (Ext. 6270). Fax: +34 968 396 213

E-mail: cromero@cebas.csic.es

Number of tables: 7

Number of figures: 4

Page count: 32 (including this one)

Research highlights:

- Reclaimed water significantly reduced total chlorophyll in grapefruit and mandarin leaves.
- Normalized Difference Vegetation Index (NDVI) was related to gas exchange variations.
- Near infrared (NIR) and red (R) domains were the best spectral indicators for both species.
- Usefulness of remote sensing for assessing diurnal changes in *Citrus* physiology was confirmed.

Effects of saline reclaimed waters and deficit irrigation on Citrus physiology assessed by UAV remote sensing.

C. Romero-Trigueros[1], P.A. Nortes[1], J.J. Alarcón[1], J.E. Hunink[2], M. Parra[1], S. Contreras[2], P. Droogers[2]. E. Nicolás[1]

[1]Departamento de Riego, Centro de Edafología y Biología Aplicada del Segura, CSIC, P.O. Box 164, Campus Universitario de Espinardo, 30100, Espinardo, Murcia, cromero@cebas.csic.es

[2]Future Water, Paseo Alfonso XIII, 48, 30203, Cartagena, Spain.

Abstract

The aim was to assess the usefulness of spectral data to detect structural and physiological changes in *Citrus* crops under water and saline stress. Multispectral images were acquired from a fixed-wing Unmanned Aerial Vehicle (UAV) while concomitant measurements of gas exchange, plant water status, leaf structural traits and chlorophyll were taken in a commercial farm located in southeast Spain with two *Citrus* species, grapefruit and mandarin irrigated for eight years with saline reclaimed water (RW) combined with regulated deficit irrigation (RDI). Measurements at leaf scale and airborne flights were carried out twice a day, at 7 and 10 GMT. Irrigation with RW decreased gas exchange and leaf dry mass per unit area (LMA) on grapefruit. However, salinity from RW resulted in an increase in pressure potential (Ψ_P) on mandarin and allowed maintaining net photosynthesis (A) and stomatal conductance (g_s) when vapour pressure deficit increased. On both crops, leaf total chlorophyll (Chl T) concentrations were significantly reduced by RW. Moreover, RDI decreased A, g_s and stem water potential (Ψ_s) on grapefruit, independently of water quality. Regarding spectral data, red wavelength (R) was significantly correlated with Chl T ($p<0.001$), except when mandarin was subjected to stressful climatic conditions (at 10 GMT); since R was influenced, in addition to Chl T, by the plant water and gas exchange status. Near infrared (NIR) was a useful indicator of Ψ_s, A and g_s on both crops. The normalized difference vegetation index (NDVI) was clearly related to gas exchange in both species and to Ψ_s only on mandarin. Finally, we combined data from both *Citrus* species and the best indicators were NIR and R. The novelty of this study was to show that diurnal changes in physiological and structural traits of *Citrus* irrigated with RW combined with RDI can be determined by multispectral images from UAVs.

Abbreviations

A: Net photosynthesis ($\mu mol \cdot m^{-2} \cdot s^{-1}$); AF: Airborne flight; C: Control treatment; Chl T: Total chlorophyll ($mg \cdot g_{FM}^{-1}$); Chl a: Chlorophyll a ($mg \cdot g_{FM}^{-1}$); Chl b: Chlorophyll b ($mg \cdot g_{FM}^{-1}$); EC: Electrical conductivity ($dS \cdot m^{-1}$); ET_c: Crop evapotranspiration ($mm \cdot month^{-1}$); ET_o: Reference evapotranspiration ($mm \cdot month^{-1}$); GMT: Greenwich Mean Time; g_s: Stomatal conductance ($mmol \cdot m^{-2} \cdot s^{-1}$); LMA: Leaf dry mass per unit area ($g \cdot m^{-2}$); NDVI: Normalized Difference Vegetation Index; NIR: Near infrared wavelength; ns: Not significant; R: Red wavelength; RDI: regulated deficit irrigation; RS: remote sensing; RW: Reclaimed water; SE: Standard error; TW: Transfer water; t_1: Time 1; t_2: Time 2; UAV: Unmanned aerial vehicle; VPD: Vapour pressure deficit (KPa); WWTP: Tertiary wastewater treatment plant. Ψ_s: Steam water potential (MPa); Ψ_π: Osmotic potential (MPa); Ψ_P: Pressure potential (MPa).

Keywords: chlorophyll; gas exchange; grapefruit; mandarin; multispectral imagery; precision agriculture; water status.

1. Introduction

Irrigation water is not always available (mainly in summer) in the semi-arid Mediterranean areas due to water scarcity (Pedrero et al., 2015). Therefore, irrigation scheduling needs to be precise, and this requires strategies to optimize irrigation water productivity (Tapsuwan et al., 2014). One technique currently in use is the regulated deficit irrigation (RDI) strategy, where water deficits are imposed only during the crop developmental stages that are least sensitive to water stress (Chalmers et al., 1981). Furthermore, current climate change predictions indicate increases in the frequency and intensity of drought periods (Garcia-Galiano et al., 2015; Stocker et al., 2013). In order to overcome this issue, the use of non-conventional water sources such as reclaimed water (RW) (RD 1620/2007) would be an alternative for farmers. On the one hand, RW can be beneficial to crops due to its concentration of macronutrients (N,P,K) (Pedrero et al., 2013); bearing in mind that an excess of them could be lost through leaching and other processes (Romero-Trigueros et al., 2014a). On the other hand, RW may have risks for agriculture because of its high concentration of salts. Therefore, inappropriate management of irrigation with RW can exacerbate problems of secondary salinization and soil degradation at the medium-long term, and finally result in negative impacts on crop physiology, growth, crop quality, etc. (Romero-Trigueros et al., 2014b).

In order to be successful, RDI strategies and improved agricultural management need a reliable characterization of the plant water status. This is achieved by measurements at leaf scale, and up-scaling this information to the canopy/field level. Measuring the spectral response of canopies is a non-destructive and rapid method to signal stress early in orchards (Jones and Vaughan, 2010). The acquisition of this information with remote sensing (RS) techniques has proven useful and cost-effective compared to more time-consuming and laborious field techniques based on leaf sampling (González-Dugo et al., 2012).

Traditional RS approaches have also a number of drawbacks: satellite imagery often suffers from issues with cloud cover, and remote sensors that are fixed on towers within crop fields are relatively expensive when data from several plots needs to be collected (Anderson and Gaston, 2013). However, in recent years, the use of unmanned airborne vehicles (UAVs) increased thanks to technological advances, cost reductions and the size of sensors. These UAVs could be operated by the farmers themselves to diagnose crop features such as water stress and then adjust their water management practices as

needed. Hence, UAV technology can fill the gap of knowledge between the leaf and the canopy by improving both the spatial and the temporal resolution of data on vegetative status (Gago et al., 2015). Nevertheless, the reliability of aerial RS approaches must be assessed with plant-truth data carried out in the field, i.e. with measurements related to plant water status (leaf water potential), gas exchange (net photosynthesis and stomatal conductance), chlorophyll content and leaf structure (Berni et al., 2009b; Contreras et al., 2014; Gago et al., 2013; González-Dugo et al., 2012, 2013; Lelong et al., 2008; Zarco-Tejada et al., 2012).

Imagery RS technologies are mainly based on canopies' wavelength reflectances in the visible, such as red, green and blue, and non-visible range of the spectrum, such as near-infrared (NIR). The remote monitoring of these specific reflectances is commonly performed using visible, multispectral and hyper-spectral cameras (Baluja et al., 2012; Zarco-Tejada et al., 2012, 2013a, 2013b). This reflectance can be used as an indicator of plant status because of its relationship with, among others, leaf pigment composition, plant biophysical or structural parameters and physiological status (Jones and Vaughan, 2010). Red wavelengths (R) (660 to 680 nm) specifically are absorbed by leaf chlorophyll (Ollinger, 2011). Because salty environments harm or reduce the functionality and content of chlorophyll in the leaves, reflectance may be proportionally reduced. In the NIR (750 to 1400 nm) domain, the spectral response depends on the multiple scattering of light inside the leaf that is mainly controlled by its internal structure, such as mesophyll thickness and water content (Bonilla et al., 2015).

Composite indices integrating data from both domains, such as the Normalized Difference Vegetation Index (NDVI), have shown positive correlations with water stress indicators (water potential and stomatal conductance) in a number of crops (Gago et al., 2015; Glenn et al., 2008). In most cases, the indicators used for this purpose are related to canopy structural changes in different days of the year or growth season, but approaches related with diurnal physiology changes along a single day are rare (Gonzalez-Dugo et al., 2015).

In the last years, research focused on checking the different vegetation indices acquired from the UAVs equipped with multi-spectral cameras and then comparing them to field-collected measurements of plant-physiological and structural increased (Berni et al., 2009a; Contreras et al., 2014; Lelong et al., 2008; Zarco-Tejada et al., 2013a,b). Drought is one of the most studied stress impulses (Baluja et al., 2012; Gago et al.,

2015; Pôcas et al., 2015; Rodriguez-Pérez et al., 2007; Stagakis et al., 2012; Zarco-Tejada et al., 2012); however, research on saline stress from RW using UAV technology is limited (Contreras et al., 2014). Besides, studies that evaluate saline and/or water stress tolerances over extended periods are scarce because of the cost and time required for extended periods of time (i.e. multiple years).

Salinity stress harms *Citrus* mainly in two ways: (1) by specific-ion toxicity and (2) by osmotic effects caused by the accumulation of salts. If the stress factor remains, changes in the leaf pigments can arise. In this sense, negative effects of salinity on the chlorophyll content have been reported in *Citrus* species (Papadakis et al., 2004; Romero-Trigueros et al., 2014b), which constitute one of the most important commercial fruit crops worldwide. The experiment reported on here is the first one to evaluate the diurnal effects of prolonged exposure (eight years) to RW and deficit irrigation on grapefruit and mandarin trees under field conditions by i) measurements of plant water status, gas exchange and chlorophyll in order to obtain the plant-truth data and ii) spectral data, acquired with an UAV, both carried out twice over the course of the day. In addition, the current work sought to assess the usefulness of multispectral imagery to determine the structural and physiological diurnal changes in *Citrus* crops under water and saline stress.

2. Materials and Methods

2.1 Site description and irrigation treatments

The experiment was conducted in 2015 in a commercial *Citrus* orchard, located at the northeast of the Region of Murcia in Campotéjar (38º07'18”N, 1°13’15”'W, 132 m above sea level) with a BSk climate by Köppen-Geiger classification (Peel et al., 2007).The 1-ha experimental plot was cultivated with i) 11 year-old 'Star Ruby’ grapefruit trees (*Citrus paradisi* Macf) grafted on Macrophylla rootstock [*Citrus Macrophylla*] planted at 6 x 4 meters and ii) 14 year-old mandarin trees (*Citrus clementina* cv Orogrande) grafted on Carrizo citrange *(Citrus sinensis* L. Obs. x *Poncirus trifoliate* L.) planted at 5 x 3.5 meters. Irrigation was scheduled on the basis of crop evapotranspiration (ET_c) accumulated during the previous week. ET_c values were estimated by multiplying reference evapotranspiration (ET_o), calculated with the Penman-Monteith methodology (Allen et al., 1998), by a monthly local crop coefficient according to Pedrero et al. (2015) for grapefruit and Nicolás et al. (2016) for mandarin. All trees received the same amount of N, P_2O_5 and K_2O through a drip irrigation

system: 215-110-150 kg ha^{-1}·$year^{-1}$ for grapefruit and 215-100-90 kg ha^{-1}·$year^{-1}$ for mandarin, respectively. Weeds were eradicated in the orchard by applying the farmers' commonly used pest control methods.

The experimental plot has been irrigated with two different water sources since 2007. In one case water was pumped from the Tajo-Segura canal (transfer water, TW) and in the other case water was pumped from the North of "Molina de Segura" tertiary wastewater treatment plant (WWTP) (reclaimed water, RW). The latter had high salt and nutrient levels (Table 1) with high electrical conductivity (EC) close to 4 $dS \cdot m^{-1}$, while for the transfer irrigation water the EC values were close to 1 $dS \cdot m^{-1}$. Saline water was automatically mixed with water from TW at the irrigation control-head to lower its EC to ≈3 $dS \cdot m^{-1}$ in order to establish a constant EC during the experiment. This high level of salinity observed in the RW was mainly due to the high concentration of Cl^- and Na (Table 1). The boron concentration in RW was considerably higher than that in TW. Moreover, higher concentrations of N, P and K were observed in RW than in TW. The pH was more basic in TW than RW (Table 1). No differences in the concentration of heavy metals were found between the irrigation water sources (data not shown).

Two irrigation treatments were established for each water source. The first treatment was a control (C) irrigated throughout the growing season to fully satisfy crop water requirements (100% ET_c). The second one was a regulated deficit irrigation (RDI) treatment irrigated similarly to C, except during the second stage of fruit development when it received half the water amount applied to the C (50% ET_c). The amount of water applied in 2015 to C was 5945 and 7531 $m^3 \cdot ha^{-1}$ for grapefruit and mandarin, respectively, while the water applied to RDI was 4875 and 6175 $m^3 \cdot ha^{-1}$ for grapefruit and mandarin, respectively. Therefore, RCD treatments saved about 18% of irrigation water in the case of both species.

The experimental design of each irrigation treatment was 4 replicate distributed following a completely randomized design. Each replicate consisted of 12 trees, organized in 3 adjacent rows. Two trees of the middle rows from each replication were used for measurements and the rest acted as guards and were excluded from the study to eliminate potential border effects. A total of 64 trees were used in this study.

2.2 Airborne imagery and image processing

A flight campaign was carried out on July 7, 2015 using a fixed-wing UAV (eBee from SenseFly) (Figure 1). Two airborne flights (AFs) were conducted at approximately 100 m of altitude over both experimental plots: the first one at 07.00 GMT (t_1) and the second at 10.00 GMT (t_2). For this study the autopilot was used, following the waypoints of a flight plan created using flight planner software (eMotion). The UAV was mounted with a GPS receiver, altimeter, wind meter and a digital camera that was electronically triggered by the autopilot system to acquire images at the correct positions. The camera used was a Canon IXUS 125 HS digital compact camera that had a 16 megapixel sensor, i.e. 4608 by 3456 pixels, and captured JPEG format images in the green, red and near infrared light range. A total of 110 images per flight were taken and processed into ortho-photos using a Structure from Motion (SfM) workflow (Lucieer et al., 2013) as implemented in the software package Agisoft PhotoScan Professional version 0.9.1.

Following previous experiences in the area (Contreras et al., 2014), the spectral data retrieved from the red (R, 600-700 nm) and near-infrared (NIR, 700-900 nm) domains were used to compute the Normalized Difference Vegetation Index (NDVI) as an indicator of the vegetation greenness. Green and dense vegetation has a strong absorption of red light due to the presence of chlorophyll, while cell walls strongly scatter (reflect and transmit) light in the NIR region. NDVI normalizes R and NIR spectral responses in order to provide a combined signal strongly related with the healthy and physiological performance of vegetation (Glenn et al., 2008). Here, NDVI was computed as:

$$NDVI = (NIR - R)/(NIR + R)$$

where NIR and R are the total radiances captured at the top of the sensor and codified as digital numbers in the near-infrared and red domains, respectively. Maps of NDVI values were computed for each experimental plot, and average values were extracted for a buffer circular area of 1m-radius centered at each tree crown in order to minimize the soil background disturbance on the overall spectral response of the crown trees.

2.3 Field data collection

Physiological and structural measurements at plant scale were conducted on July 7, 2015, the same date as UAV flights, and after two weeks of the beginning of deficit

irrigation in this season, in order to obtain the plant-truth data. They were carried out twice a day: at 07.00 GMT (t_1) and at 10.00 GMT (t_2), coinciding with the AFs described in section 2.2.

Leaf-scale gas-exchange parameters (net photosynthesis, A, and stomatal conductance, g_s) and stem water potential (Ψ_s) were determined on eight fully-expanded leaves from the mid-shoot area of each tree per treatment (two leaves from each replicate).

A and g_s were determined with a portable photosynthesis system (LI-6400 Li-Cor, Lincoln, Nebraska, USA) equipped with a clear chamber bottom (6400-08) and a LICOR 6400-01 CO_2 injector using a 6 cm^2 leaf cuvette. The CO_2 concentration in the cuvette was maintained at 400 $\mu mol \cdot mol^{-1}$ (≈ambient concentration). Measurements were performed at saturating light intensity (1200 $\mu mol \cdot m^{-2} \cdot s^{-1}$) and at ambient air temperature and relative humidity. The air flow was set to 300 $mL \cdot min^{-1}$. Ψ_s was measured using a pressure chamber (model 3000; Soil Moisture Equipment Corp., California, USA), according to Scholander et al. (1965), in leaves close to the trunk which had been bagged within foil-covered aluminum envelopes at least 2 h before (Shackel et al., 1997). Leaves from the Ψ_s measurements at t_2 were frozen in liquid nitrogen (-196 ºC) and stored at -30 ºC till analysis. After thawing, osmotic potential (Ψ_π) was measured in the extracted sap, according to Gucci et al. (1991), using a WESCOR 5520 vapour pressure osmometer (Wescor Inc., Logan, UT, USA). Pressure potential (Ψ_P) was calculated as the difference between Ψ_s and Ψ_π.

Leaf area was determined using an area meter (LI-3100 Leaf Area Meter, Li-Cor, Lincoln, Nebraska, USA**)** in twenty leaves per tree collected from the two central trees of each replicate per treatment in the early morning and transported in refrigerated plastic bags to the laboratory**.** Then, leaves were washed with running tap water followed by rinsing in distilled (Desta, 2014) water and left to drain on a filter paper before being oven dried for at least 2 days at 65 ºC. Later, we determined the dry weight to calculate leaf dry mass per unit area (LMA, $g \cdot m^{-2}$).

Regarding phytotoxic elements, sodium and boron were determined by Inductively Coupled Plasma mass spectrometry (ICP- ICAP 6500 DUO Thermo, Cambridge, UK) and chloride anion by ion chromatography with a Chromatograph Metrohm (Switzerland) in the dried leaves which were ground and digested with a mix of acid nitric (4 mL) and hydrogen peroxide (1 mL).

Finally, leaf chlorophyll determination was carried out as described in Romero-Trigueros et al. (2014b).

2.4 Statistical analysis

A weighted analysis of variance (ANOVA) followed by Tukey ´s test ($P \leq 0.05$) were used for assessing differences among treatments. Linear regressions among variables measured in the field and spectral data were calculated. Pearson correlation coefficients were used to assess the significance of these relationships. All statistical analyses were performed using SPSS (vers. 23.0 for Windows, SPSS Inc., Chicago, IL, USA).

3. Results and Discussion

3.1 Plant water status and leaf structural traits

We considered the data presented in this section as truth-plant data because they are field-collected-leaf measurements. Table 2 shows some climate variables for July 7, 2015: vapour pressure deficit, mean temperature and average radiance increased from t_1 to t_2, as expected.

Plant water status

Stem water potential (Ψ_s) was not influenced by salinity from RW in any of the crops (Figure 2), in agreement with the results found by Nicolás et al. (2016) for mandarin trees. Nevertheless, plant-water relations are proven to be affected by water quality (Paranychianakis et al., 2004). Regarding RDI, there were no significant differences between treatments of grapefruit trees at t_1. However, at t_2 Ψ_s of the RDI treatments declined significantly with respect to that of the C treatments: 15% for TW treatments and 11% for RW treatments, as expected. Short-term water deficits may affect plant growth processes and therefore monitoring of water stress is critical not only for early detection of stress, but also for applying RDI strategies (Fereres and Soriano, 2007) with the degree of precision needed. On mandarin trees, the more negative Ψ_s values at t_1 were observed for the C trees for both TW and RW treatments (TW-C and RW-C). This was probably because the well-irrigated trees had at the end of winter 2014 greater plant canopies than the trees under RDI, thus absorbing more water from the soil profile with a consequent lower water potential in the morning. The measurements were carried out only two weeks after the initiation of RDI.

On the one hand, both salinity and water stress in grapefruit resulted in a decrease of $\Psi_{\pi,}$ with a slight increase in Ψ_P, although in this case no significant differences were observed between treatments (Table 3). On the other hand, in mandarin only the RW treatments (RW-C and RW-RDI) showed a Ψ_π more negative than TW treatments and, in this case it resulted in a significant rise in Ψ_P, similar to findings by Aksoy et al. (1998) and Gimeno et al. (2009) for mandarin and lemon trees, respectively. It is known that when Ψ_P of ´*Carrizo Citrange*´ under saline conditions is similar to or higher than that of C trees, Cl^- and Na accumulation represent important osmotic adjustment processes and not a significant toxicity effect (Pérez-Pérez et al., 2007). Therefore, according to Aksoy et al. (1998), the response of different *Citrus* rootstocks under saline conditions is not always similar since in our case salinity from RW only increased the leaf turgor in mandarin trees and not in grapefruit trees.

Gas exchange parameters

In the case of grapefruit, both water and saline stress decreased A and g_s (Table 4), in agreement with observations by other authors (Anjum, 2008; Hussain et al., 2012; Melgar, 2008). Stomatal conductance in particularly is considered a suitable parameter to assess plant water stress (Flexas et al., 2002). A reduction of this parameter in well-irrigated, but salt-stressed *Citrus* leaves has also been associated with the specific toxicity of Cl^- and/or Na (Levy and Syvertsen, 2004), as probably happened in the case of the RW-C.

On mandarin trees at t_1, RDI treatments showed A values slightly higher than their corresponding C treatments, but these differences were not significant. This behaviour responded to Ψ_s (Figure 2). Besides, there was stomatal closure in RW-C with respect to the rest of the treatments (Table 4). In this sense, Ψ_s regulated physiological processes (Gomes et al., 2004) and induced stomatal closure which reduced A. At t_2, unlike with grapefruit, both parameters decreased only in TW-RDI, and not in RW treatments. As mentioned above, one of the main plant adaptations to osmotic stress, e.g. from saline water, is osmotic adjustment which maintains the positive leaf turgor required to keep stomata open and sustain gas exchange (García-Sánchez and Syvertsen, 2006) as occurred in RW treatments. This response has already been described for *Citrus*, but is rootstock dependent (García-Tejero et al., 2010) since it determines the tolerance or sensitivity to different abiotic stresses, including salinity (Gimeno et al., 2012; Navarro et al., 2011). Our results for example showed that mandarin trees, grafted on ´*Carrizo*

citrange´, increased their Ψ_P when they were irrigated with RW and, for that reason, gas exchange was unaffected; however, grapefruit trees, grafted on *Macrophylla* rootstock, responded differently (Table 4).

Finally, *Citrus* trees grown in semi-arid areas are affected by high VPD that induce a continuous decline in g_s and A from the early morning hours, even when trees are well-irrigated (Villalobos et al., 2008). In our study, grapefruit trees showed A and g_s levels higher than mandarin trees and the lower reduction of both parameters from t_1 to t_2 was in grapefruit trees: the RW-RDI treatment of grapefruit was the most affected (reduction of 44 and 42% for A and g_s, respectively) caused by a water stress and a Na, Cl^- and B accumulation (Table 5). In the case of mandarin, TW-RDI showed the highest decline (79 and 60% for A and g_s, respectively).

Leaf structural traits: leaf dry mass, phytotoxic elements and chlorophyll.

LMA is positively related to leaf photosynthetic capacity (Niinemets, 1999), hence grapefruit trees presented higher values of LMA than mandarin trees (Table 5), as expected from gas exchange measurements. There were also significant differences between treatments: the highest LMA values were observed in TW treatments for grapefruit trees and in RW-RDI for mandarin (Table 5).

Regarding phytotoxic elements (Table 5), RW-C treatment showed Cl^-, Na and B levels significantly higher than TW treatments in both crops, except to the B in mandarin. In agreement with the phytotoxic thresholds reported by Romero-Trigueros et al. (2014b), in our study the Na limit was not exceeded by any treatment, Cl^- only by RW-C of mandarin and B by both RW treatments on grapefruit and RW-RDI on mandarin.

Moreover, differences in leaf chlorophyll content can be an indicator of photosynthetic capacity and degree of stress (Wu et al., 2008). In addition, the coefficient Chl a/Chl b (Coef a/b) can be used as an index to characterize the plant physiological status. In our study, RW treatments of both crops showed the lowest values of total chlorophyll, Chl *T* (Figure 3) and the highest values of Coef a/b, in accordance with Bondada and Syvertsen (2003). Only in RW treatments of mandarin the Coef a/b increased from t_1 to t_2 (Figure 3C and 3D) due to a decrease in Chl b since increments in radiance destroy the Chl b in greater proportion than Chl a due to the fact that photosystem II, which is rich in Chl b, becomes more unstable (Casierra-Posada, 2007).

3.2 Spectral indicators in *Citrus* species

In general, we observed that reflectance in the NIR region was about 7% higher in Control grapefruit than in Control mandarin trees whereas the reflectance values in the R wavelength were about 3% lower in control grapefruit than in Control mandarin trees at t_1. No differences were detected at t_2 between species. It is noticeable that R and NIR reflectance decreased from t_1 to t_2 within all mandarin and grapefruit treatments due to changes in climatic conditions (solar radiation, air temperature, VPD, etc.).

Grapefruit

At t_1, trees under water and salt stress (TW-RDI, RW-C and RW-RDI) showed a significant increase in the reflectance on the R domain with respect to TW-C (Table 6A). This is in contrast with what Contreras et al. (2014) found for the same plot at the beginning of the RW application in 2009. This increase in R responds to the observed decrease in Chl T in those treatments (Figure 3A). On the contrary, no significant differences between treatments were found in the NIR region. The NDVI was significantly higher in TW than RW treatments (Table 6A). Similar results were obtained by Contreras et al. (2014). At t_2, only trees irrigated with RW showed an increase in the R domain, coinciding again with Chl T (Figure 3A). NIR reflectance in this second AF was significantly lower in both RDI treatments (TW-RDI and RW-RDI) but not in RW-C (Table 6A), in accordance with lower Ψ_s levels (Figure 2A).

Mandarin

At t_1, the highest R values were observed in RW treatments. The RW-RDI had the biggest effect, probably as a result of the low chlorophyll concentration (Figure 3B). Regarding the NIR region, trees under deficit irrigation (RDI treatments) had higher values than C trees, in accordance with Ψ_s data (Figure 2B). Moreover, in contrast to grapefruit, the trees with significantly higher NDVI values were those in the C treatments, regardless of water quality. At t_2, R increased only with TW-RDI (Table 6B) and not with RW treatments also, as expected it would do in relation to chlorophyll decreases (Figure 3B).

It is thus worth highlighting that the Ψ_P increase in RW treatments (Table 3), due to a low Ψ_π driven by Cl^- and Na from RW, likely interfered with R reflectance. Finally, there were no significant differences among treatments for NIR.

3.3 Correlations between spectral indicators and plant water status and leaf structural traits.

Red domain (R)

On grapefruit trees (Table 7A), the R domain was significantly correlated with Chl T and Coef a/b ($p<0.01$ and $p<0.05$, respectively) as expected according to the data shown in sections 3.1 and 3.2. This correlation was negative since R reflectance is lower with increasing chlorophyll. Sims and Gamon (2002) and Ollinger (2011) demonstrated that the R domain was linked to the photosynthetic leaf pigments across a wide range of species. Because of important physiological roles of leaf chlorophyll and its strong absorbance properties, it is important have corroborated that the method here evaluate using UAVs is a useful and effective tool to estimate Chl T from grapefruit canopy reflectance and that avoids destructive laboratory methods. Moreover, the R domain was also significantly linked to Ψ_P. This was associated to the fact that absorbance includes light absorbed by pigments, as we observed with R absorbance by Chl T, but maybe also by other leaf constituents (Kokaly et al., 2009) such as those associated with the increased turgor.

On mandarin trees, the R domain was significantly related to Ψ_s, A and g_s according to Sims and Gamon (2002). To the contrary, no significant correlation between the R and Chl T was observed since the R values found in the RW treatments were lower than expected, as the Chl T concentration at t_2 (Figure 3B). Consequently, under high VPD conditions reflectance of mandarin trees (at t_2) was stronger influenced by gas exchange, Ψ_π and Ψ_P than by chlorophyll (RW treatments showed the highest Ψ_π and Ψ_P, Table 3).

Near infrared domain (NIR)

The biophysical basis for high leaf-level reflectance in the NIR region is provided by (Ollinger, 2011). It is related to the likelihood of photons being scattered from the point of entry into the leaf because absorption by leaf constituents is either small or altogether absent (Merzlyak et al., 2002). In our study, NIR for both grapefruit and mandarin trees was positively linked to Ψ_s and consequently with gas exchange parameters, as we expected from the results of sections 3.1 and 3.2. High values of net photosynthesis (A) correlated with high NIR values, likely as a result of scattering in the NIR region caused by high CO_2 levels in leaves (Ollinger, 2011).

NDVI index

The NDVI index for grapefruit trees had a direct relationship with A and g_s in accordance with data reported by Baluja et al. (2012) and Gago et al. (2015) for vineyards, and Zarco-Tejada et al. (2012) for *Citrus*. The NDVI for mandarin trees correlated well with Ψ_s, in agreement with the findings of Baluja et al. (2012). NDVI and other vegetation indices proposed to monitor vegetation dynamics are considered *structural* indices related to plant vigor (Dobrowski et al., 2005; Gago et al., 2015; González-Dugo et al., 2015; Zarco-Tejada et al., 2013b) as they track changes in canopy structure but have little or no sensitivity to short-term leaf physiological changes which are independent of canopy structure according to Haboudane et al. (2004). However, the current work showed that in case of *Citrus*, NDVI responds to short-term changes in gas exchange and Ψ_s. Thus, we can confirm that NDVI can be sensitive in *Citrus* to diurnal physiological changes induced by variations in environmental conditions throughout the day and not only tracks the effects in the long term as other authors indicated (Dobrowski et al., 2005; Zarco-Tejada et al., 2013c). Similar conclusions were obtained Baluja et al. (2012) for vineyard crop.

Best indicators across species

Bearing in mind data from both species together (Figure 4), NIR was significantly correlated with Ψ_s ($p<0.005$) and R with Chl T ($p<0.005$). For the last one, it was necessary to eliminate the point from the RW treatment at t_2 of mandarin due to –as was mentioned above- when mandarin trees were under high values of VPD (at t_2), the R domain is more influenced by gas exchange, Ψ_π and Ψ_P, than by chlorophyll. Therefore,

449 we considered the NIR and R spectral indicators as the best related to the parameters
450 measured at the leaf scale for *Citrus* crops.

451 **4. Conclusions**

452 This study assessed the effects of eight years of irrigation with RW and deficit irrigation
453 on grapefruit and mandarin trees on a diurnal basis. The results suggest that on
454 grapefruit trees the water potential was affected by water stress (RDI) but not by saline
455 stress when trees were well irrigated with RW. Gas exchange was reduced by both
456 stresses. The water potential of mandarin trees was not affected by any treatment and
457 gas exchange was only reduced by RDI with TW. The total chlorophyll of both crops
458 decreased with RW treatments.

459 Regarding spectral data, for grapefruit, R wavelength values increased with RW
460 treatments, consistent with chlorophyll data, and the NDVI levels decreased at 07.00
461 GMT since gas exchange also declined. The NIR region was affected mainly by deficit
462 irrigation, regardless water quality, in the second airborne flight. For mandarin, R
463 domain increased with declining of chlorophyll in RW treatments. However, when
464 climatic conditions were more stressful, R was influenced mainly by the increasing leaf
465 turgor and gas exchange. Therefore, the response in R was attributed to stress-induced
466 declines in leaf chlorophyll. But when VPD was too high, R could detect physiological
467 changes in other parameters and responded in a shorter term than those related
468 exclusively with the chlorophyll synthesis. NIR was linked to deficit irrigation
469 treatments and NDVI only increased under well irrigated conditions, regardless of water
470 quality.

471 Because all of the above, we obtained significant correlations between: i) For grapefruit:
472 R with chlorophyll and potential turgor; NIR with Ψ_s and gas exchange (A and g_s); and
473 NDVI with gas exchange. ii) For mandarin: R correlated with chlorophyll only at the
474 first hour of the morning; NIR with stem water potential and gas exchange, as in
475 grapefruit, and NDVI with stem water potential.

476 We conclude the following: The statistical analyses of field data and remote sensing
477 data, derived from multispectral imagery using an UAV, confirms the feasibility of
478 applying the proposed methods to assess physiological and structural properties of
479 *Citrus* under water and saline stress.

480

Acknowledgment

This study was supported by two CICYT (AGL2010-17553 and AGL2013-49047-C2-515 2-R) projects and SIRRIMED (KBBE-2009-1-2-03, PROPOSAL N◦245159) project. We are also grateful to SENECA–Excelencia Científica (19903/GERM/15) for providing funds for this research.

References

Aksoy, U., Hepaksoy, S., Can, H.Z., Anaç, S., Ul, M.A., Dorsan, F., Anaç, D., Okur, B., Kiliç, C., 1998. The effect of rootstock on leaf characteristics and physiological response of satsuma mandarins under saline conditions. Acta Hortic. 513, 169-176. doi: 10.17660/ActaHortic.1998.513.19.http://dx.doi.org/10.17660/ActaHortic.1998.513.19

Allen, R.G., Pereira, L.S., Raes, D., Smith, M., 1998. Crop evapotranspiration-guidelines for computing crop water requirements. FAO Irrig. Drain. 56, 15-27.

Anderson, K., Gaston, K.J., 2013. Lightweight unmanned aerial vehicles will revolutionize spatial ecology. Front. Ecol. Environ. 11(3), 138–146.

Anjum, M.A., 2008. Effect of NaCl concentrations in irrigation water on growth and polyamine metabolism in two citrus rootstocks with different levels of salinity tolerance. Acta Physiol. Plant. 30, 43-52.

Baluja, J., Diago, M.P., Balda, P., Zorer, R., Meggio, F., Morales, F., Tardaguila, J., 2012. Assessment of vineyard water status variability by thermal and multispectral imagery using an unmanned aerial vehicle (UAV). Irrig. Sci. 30(6), 511-522.

Berni, J.A.J., Zarco-Tejada, P.J., Sepulcre-Cantó, G., Fereres, E., Villalobos, F., 2009a. Mapping canopy conductance and CWSI in olive orchards using high resolution thermal remote sensing imagery. Remote Sens. Environ. 113(11), 2380-2388.

Berni, J.A.J., Zarco-Tejada, P.J., Suárez, L., Fereres, E., 2009b. Thermal and narrow band multispectral remote sensing for vegetation monitoring from an unmanned aerial vehicle. Geosci. Remote Sens. IEEE Trans. 47(3), 722–738. http://dx.doi.org/10.1109/TGRS.2008.2010457.

509 Bondada, B.R., and Syvertsen, J.P., 2003. Leaf chlorophyll, net gas exchange and
510 chloroplast ultrastructure in citrus leaves of different nitrogen status. Tree Physiol.
511 23(8), 553-559.

512 Bonilla, I., Martínez, F., Martínez-Casasnovas, J.A., 2015. Vine vigor, yield and grape
513 quality assessment by airborne remote sensing over three years: Analysis of unexpected
514 relationships in cv. Tempranillo. Span. J. Agric. Res. 13(2), e0903, 8 pages. eISSN:
515 2171-9292. http://dx.doi.org/10.5424/sjar/2015132-7809.

516 Casierra-Posada, F., Ávila-León, O.F., Riascos-Ortíz, D.H., 2012. Diurnal changes in
517 photosynthetic pigments content in sun and shade marigold leaves. Temas Agrarios. 17,
518 60- 71.Chalmers, D.J., Mitchell, P.D., Van Heek, L., 1981. Control of peach tree growth
519 and productivity by regulated water supply, tree density and summer pruning. J. Am.
520 Soc. Hort. Sci. 106, 307–312.

521 Contreras, S., Pérez-Cutillas, P., Santoni, C.S., Romero-Trigueros, C., Pedrero, F.,
522 Alarcón, J.J., 2014. Effets of reclaimed waters of spectral properties and leaf traits of
523 citrus orchards. Water Environ. Res. 86, 2242-2250.

524 Desta, K.G., 2014. Washing Plant Tissue Samples for Mineral Nutrient Analysis.
525 Washington State University, USA. Extension fact sheet FS134E.

526 Dobrowski, S.Z., Pusknik, J.C., Zarco-Tejada, P.J., Ustin, S.L., 2005. Simple
527 reflectance indices track heat and water stress induced changes in steady state
528 chlorophyll fluorescence. Remote Sens. Environ. 97(3), 403-414.

529 Fereres, E., Soriano, M., 2007. Deficit irrigation for reducing agricultural water use. J.
530 Exp. Bot. 58, 147-159.

531 Flexas, J., Bota, J., Escalona, J.M., Sampol, B., Medrano, H., 2002. Effects of drought
532 on photosynthesis and electron transport rate regulation in grapevine. Plant Cell
533 Environ. 22, 39-48.

534 Gago, J., Martorell, S., Tomás, M., Pou, A., Millán, B., Ramón, J., Ruiz, M., Sánchez,
535 R., Galmés, J., Conesa, M.A., Cuxart, J., Tardáguila, J., Ribas-Carbó, M., Flexas, J.,
536 Medrano, H., Escalona, J.M., 2013. High-resolution aerial thermal imagery for plant
537 water status assessment in vineyards using a multicopter-RPAS. In: "VII Congreso
538 Ibérico de Agroingeniería y Ciencias Hortícolas. Sociedades Españolas de
539 Agroingeniería y de Ciencias Hortícolas, y las Sociedades Portuguesas de Horticultura y

la Sección Especializada de Ingeniería Rural de la Sociedad de Ciencias Agrarias de Portugal.", Madrid, España. Poster.

Gago, J., Douthe, C., Coopman, R.E., Gallego, P.P., Ribas-Carbo, M., Flexas, J., Escalona, J., Medrano, H., 2015. UAVs challenge to assess water stress for sustainable agriculture. Agric. Water Manage. 153, 9-19.

Garcia-Galiano, S.G., Olmos-Giménez, P., Giraldo-Osorio, J.D., 2015. Assessing Nonstationary Spatial Patterns of Extreme Droughts from Long-Term High-Resolution Observational Dataset on a Semiarid Basin (Spain). Water. 7(10), 5458-5473. doi:10.3390/w7105458

García-Sánchez, F., Syvertsen, J.P., 2006. Salinity reduces growth, gas exchange, chlorophyll and nutrient concentrations in diploid sour orange and related allotetraploid somatic hybrids. J. Hort. Sci. Biotechnol. 77, 379-386.

García-Tejero, I., Jiménez-Bocanegra, J.A., Martínez, G., Romero, R., Durán-Zuazo, V,H., Muriel-Fernández, J.L., 2010. Positive impact of regulated deficit irrigation on yield and fruit quality in a commercial citrus orchard. Agric. Water Manage. 97, 614-622.

Geoghegan-Quin, M., 2013. Role of Research & Innovation in Agriculture. European Commission-SPEECH/13/505. http://europa.eu/rapid/press-releaseSPEECH-13-505 en.htm

Gimeno, V., Syvertsen, J. P., Nieves, M., Simón, I., Martínez, V., Garcia-Sanchez, F., 2009. Orange varieties as interstocks increase the salt tolerance of lemon trees. J. Hortic. Sci. Biotechnol. 84(6), 625-631. doi: 10.1080/14620316.2009.11512577.

Gimeno, V., Simón, I., Nieves, M., Martínez, V., Cámara-Zapata, J.M., García, A.L., García-Sánchez, F., 2012. The physiological and nutritional responses to an excess of boron by Verna lemon trees that were grafted on four contrasting rootstocks. Trees-Struc. Funct. 26(5), 1513-1526.

Glenn, E.P., Huete, A.R., Nagler, P.L., Nelson, S.G., 2008. Relationship between Remotely-Sensed Vegetation Indices, Canopy Attributes and Plant Physiological Processes: What Vegetation Indices Can and Cannot Tell Us about the Landscape. Sensors. 8, 2136–2160.

570 Gomes, M.M., Lagoa, A.M.M.A., Medina, C.L., Machado, E.C., Machado, M.A., 2004.
571 Interactions between leaf water potential, stomatal conductance and abscisicacid content
572 of orange trees submitted to drought stress. Braz. J. Plant. Physiol. 13(3), 155–161.

573 González-Dugo, V., Zarco-Tejada, P., Berni, J.A., Suárez, L., Goldhamer, D., Fereres,
574 E., 2012. Almond tree canopy temperature reveals intra-crown variability that is water
575 stress-dependent. Agric. Forest. Meteorol. 154, 156–165.

576 González-Dugo, V., Zarco-Tejada, P., Nicolás, E., Nortes, P.A., Alarcón, J.J.,
577 Intrigliolo, D.S., Fereres, E., 2013. Using high resolution UAV thermal imagery to
578 assess the variability in the water status of five fruit tree species within a commercial
579 orchard. Precis. Agric. 14(6), 660–678.

580 Gonzalez-Dugo, V., Hernandez, P., Solis, I., Zarco-Tejada, P.J., 2015. Using High-
581 Resolution Hyperspectral and Thermal Airborne Imagery to Assess Physiological
582 Condition in the Context of Wheat Phenotyping. Remote Sens. 7, 13586-13605.

583 Gucci, R., Xiloyannis, C., Flore, J.A., 1991. Gas exchange parameters water relations
584 and carbohydrate partitioning in leaves of field-grown Prunus domestica following fruit
585 removal. Physiol. Plant. 83, 497–505.

586 Haboudane, D., Miller, J.R., Pattey, E., Zarco-Tejada, P.J., Strachan, I., 2004.
587 Hyperspectral vegetation indices and novel algorithms for predicting green LAI of crop
588 canopies: Modeling and validation in the context of precision agriculture. Remote Sens.
589 Environ. 90(3), 337-352.

590 Hussain, S., Luro, F., Costantino, G., Ollitrault, P., Morillon, R., 2012. Physiological
591 analysis of salt stress behavior of citrus species and genera: Low chloride accumulation
592 as an indicator of salt tolerance. South Afr. J. Bot. 81, 103-112.

593 Jones, H.G., Vaughan, R.A., 2010. Remote Sensing of Vegetation: Principles,
594 Techniques and Applications. Oxford University Press Inc., New York.

595 Kokaly, R.F., Asner, G.P., Ollinger, S.V., Martin, M.E., Wessman, C.A., 2009.
596 Characterizing canopy biochemistry from imaging spectroscopy and its application to
597 ecosystem studies. Remote Sens Environ. 113, 78-91. doi: 10.1016/j.rse.2008.10.018.

598 Lelong, C.C., Burger, P., Jubelin, G., Roux, B., Labbé, S., Baret, F., 2008. Assessment
599 of unmanned aerial vehicles imagery for quantitative monitoring of wheat crop in small
600 plots. Sensor. 8(5), 3557-3585. http://dx.doi.org/10.3390/s8053557.

601 Levy, Y., Syvertsen, J.P., 2004. Irrigation water quality and salinity effects in citrus
602 trees. Hortic. Rev. 30, 37-82.

603 Lucieer, S.M., Jong, D., Turner, D., 2013. Mapping landslide displacements using
604 Structure from Motion (SfM) and image correlation of multi-temporal UAV
605 photography, Prog. Phys. Geogr. 38(1), 97–116. doi:10.1177/0309133313515293.

606 Melgar, J.C., 2008. Leaf gas exchange, water relations, nutrient content and growth in
607 citrus and olive seedlings under salinity. Biol. Plant. 52, 385-390.

608 Merzlyak, M.N., Chivkunova, O.B., Melo, T.B., Naqvi, K.R., 2002. Does a leaf absorb
609 radiation in the near infrared (780-900 nm) region? A new approach to quantifying
610 optical reflection, absorption and transmission of leaves. Photosyn. Res. 72(3), 263-270.

611 Navarro, J.M., García-Olmos, B., Andujar, S., Rodríguez-Morán, M., Moreno, M.,
612 Porras, I., 2011. Effects of calcium on growth and nutritional state of citrus seedlings
613 under NaCl stress. Acta Hortic. 922, 55-60.

614 Nicolás, E., Alarcón, J.J, Mounzer, O., Pedrero, F., Nortes, P.A., Alcobendas, R.,
615 Romero-Trigueros, C., Bayona, J.M., Maestre-Valero, J.F., 2016. Long-term
616 physiological and agronomic responses of mandarin trees to irrigation with saline
617 reclaimed water. Agric. Water Manage. 166, 1-8.

618 Niinemets, U., 1999. Research review. Components of leaf dry mass per area-thickness
619 and density-alter leaf photosynthetic capacity in reverse directions in woody plants.
620 New Phytol. 144, 35-47.

621 Ollinger, S.V., 2011. Sources of Variability in Canopy Reflectance and the Convergent
622 Properties of Plants. New Phytol. 189, 375–394.

623 Papadakis, I.E., Dimassi, K.N., Bosabalidis, A.M., Therios, I.N., Giannakoula, A.,
624 2004. Effects of B excess on some physiological and anatomical parameters of
625 'Navelina' orange plants grafted on two rootstocks. Environ. Exp. Bot. 51, 247-257.

626 Paranychianakis, N.V., Chartzoulakis, K.S., Angelakis, A.N., 2004. Influence
627 ofrootstock, irrigation level and recycled water on water relations and leaf gas exchange
628 of Soultanina grapevines. Environ. Exp. Bot. 52, 185–198.

629 Pedrero, F., Mounzer, O., Alarcón, J.J., Bayona, J.M., Nicolás, E., 2013. The viability
630 of irrigating mandarin trees with saline reclaimed water in a semi-arid mediterranean
631 region: a preliminary assessment. Irrig. Sci. 31(4), 759-768.

Pedrero, F., Maestre-Valero, J.F., Mounzer, O., Nortes, P.A., Alcobendas, R., Romero-Trigueros, R., Bayona, J.M., Alarcón, J.J., Nicolás, E., 2015. Response of young 'Star Ruby' grapefruit trees to regulated deficit irrigation with saline reclaimed water. Agric. Water Manage. 158, 51-60.

Peel, M.C., Finlayson, B.L., McMahon, T.A., 2007. Updated world map of the Köppen-Geiger climate classification. Hydrol. Earth Syst. Sc. 11, 1633–1644.

Pérez-Pérez, J.G., Syvertsen, J.P., Botía, P., García-Sánchez, F., 2007. Leaf Water Relations and Net Gas Exchange Responses of Salinized Carrizo Citrange Seedlings during Drought Stress and Recovery. Ann. Bot. 100(2), 335-345.

Pôcas, I., Rodrigues, A., Gonçalvez, S., Costa, P.M., Gonçalves, I., Pereira, L.S., Cunha, M., 2015. Predicting grapevine water status based on hyperspectral reflectance vegetation indices. Remote Sens. 7, 16460-16479. doi: 10.3390/rs71215835.

Rodriguez-Pérez, J.R., Riaño, D., Carlisle, E., Ustin, S., Smart, D.R., 2007. Evaluation of hyperspectral reflectance indexes to detect grapevine water status in vineyards. Am. J. Enol. Vitic. 58, 302-317.

Romero-Trigueros, C., Nortes, P.A., Alarcón. J.J., Nicolás, E., 2014a. Determination of ^{15}N stable isotope natural abundances for assessing the use of saline reclaimed water in grapefruit. Environ. Eng. Manag. J. 13(10), 2525-2530.

Romero-Trigueros, C., Nortes, P.A., Pedrero, F., Mounzer, O., Alarcón, J.J., Bayona, J.M., Nicolás, E., 2014b. Assessment of the sustainability of using saline reclaimed water in grapefruit in medium to long term. Span. J. Agric. Res. 12(4), 1137-1148.

Scholander, P.F., Hammel, H.T., Bradstreet, E.D., Hemmingsen, E.A., 1965. Sap pressure in vascular plants. Science. 148, 339-434

Shackel, K., Ahmadi, H., Biasi, W., Buchner, R., Goldhamer, D., Gurusinghe, S., Hasey, J., Kester, D., Krueger, B., Lampinen, B., McGourty, G., Micke, W., Mitcham, E., Olson, B., Pelletrau, K., Philips, H. Ramos, D., Schwankl, L., Sibbett, S., Snyder, R., Southwick, S., Stevenson, M., Thorpe, M., Weinbaum, S., Yeager, J., 1997. Plant water status as an index of irrigation need in deciduous fruit trees. Hort. Technol. 7(1), 23–29.

Sims, D.A., Gamon, J.A., 2002. Relationships between leaf pigment content and spectral reflectance across a wide range of Species, Leaf structures and developmental stages. Remote Sens. Environ. 81, 337-354.

663 Stagakis, S., González-Dugo, V., Cid, P., Guillén-Climent, M.L., Zarco-Tejada, P.J.,
664 2012. Monitoring wáter stress and fruit quality in an orange orchard under regulated
665 déficit irrigation using narrox-band structural and physiological remote sensing indices.
666 J. Photogramm. Remote Sens. 71, 47-61.

667 Stocker, T.F., Qin, D., Plattner, G.K., Tignor, M., Allen, S.K., Boschung, J., Nauels,
668 A.,Xia, Y., Bex, V., Midgley, P.M., 2013. IPCC Climate Change 2013: The Physical
669 Science Basis. Contribution of Working Group I to the Fifth Assessment Report of the
670 Intergovernmental Panel on Climate Change. Cambridge University Press, Cambridge,
671 UK/New York, NY, USA.

672 Tapsuwan, S., Hunink, J.E., Alcon, F., Mertens-Palomares, A., Baille, A., 2014.
673 Assessing the design of a model-based irrigation advisory bulletin: the importance of
674 end-user participation. Irrig Drain. 64, 228–240. doi: 10.1002/ird.1887.

675 Villalobos, F.J., Testi, L., Moreno-Perez, M.F., 2008. Evaporation and canopy
676 conductance of citrus orchard. Agric. Water Manage. 96(4), 565-573.

677 Wu, C., Niu, Z., Tang, Q., Huang, W., 2008. Estimating chlorophyll content from
678 hyperspectral vegetation indices: Modeling and validation. Agric. For Meteorol. 148,
679 1230-1241.

680 Zarco-Tejada, P.J., González-Dugo, V., Berni, J.A., 2012. Fluorescence, temperature
681 and narrow-band indices acquired from a UAV platform for water stress detection using
682 a micro-hyperspectral imager and a thermal camera. Remote Sens. Environ. 117, 322-
683 337.

684 Zarco-Tejada, P.J., Guillén-Climent, M.L., Hernández-Clemente, R., Catalina, A.,
685 González, M.R., Martín, P., 2013a. Estimating leaf carotenoid content in vine-yards
686 using high resolution hyperspectral imagery acquired from an unmanned aerial vehicle
687 (UAV). Agric. For. Meteorol. 171, 281-294.

688 Zarco-Tejada, P.J., González-Dugo, V., Williams, L.E., Suárez, L., Berni, J.A.J.,
689 Goldhamer, D., Fereres, E., 2013b. A PRI-based water stress index combining structural
690 and chlorophyll effects: assessment using diurnal narrow-band air-borne imagery and
691 the CWSI thermal index. Remote Sens. Environ. 138, 38-50.

692 Zarco-Tejada, P.J., Morales, A., Testi, L., Villalobos, F.J., 2013c. Spatio-temporal
693 patterns of chlorophyll fluorescence and physiological and structural indices acquired

from hyperspectral imagery as compared with carbon fluxes measured with eddy covariance. Remote Sens. Environ. 133, 102-115.

Table 1. Physical and chemical properties for Tajo-Segura transfer water and reclaimed water in 2015.

Property	Units	TW	RW
EC	**dS m^{-1}**	1.00±0.01	3.21±0.20
pH		8.41±0.09	7.70±0.10
Ca	**meq·L^{-1}**	1.99±0.10	3.58±0.20
Mg	**meq·L^{-1}**	1.58±0.10	3.92±0.30
K	**mg·L^{-1}**	3.65±1.40	38.94±1.40
Na	**meq·L^{-1}**	1.86±0.20	18.30±1.20
B	**mg·L^{-1}**	0.10±0.01	0.66±0.04
Cl^-	**meq· L^{-1}**	3.15±0.40	20.10±3.01
NO_3^-	**mg·L^{-1}**	7.70±3.60	25.42±10.6
PO_4^{---}	**mg·L^{-1}**	0.31±0.02	1.73±0.70
SO_4^{--}	**meq·L^{-1}**	5.90±0.50	17.20±3.40

Values are averages ± SE of 12 individual samples taken throughout the crop cycle. EC: electrical conductivity (dS·m^{-1}); RW: reclaimed water; TW: transfer water.

Table 2. Vapour pressure deficit, mean temperature and average radiation recorded at the agrometeorological station of Campotéjar (Molina de Segura) at different airborne flights.

	t_1	t_2
VPD (kPa)	3.28	6.19
Temperature (ºC)	30.05	38.54
Radiation (W·m^{-2})	608.97	954.67

t_1: 07.00 GMT; t_2: 10.00 GMT; VPD: Vapour pressure deficit.

739 **Table 3. Osmotic and pressure potential values of grapefruit and mandarin at 10.00 GMT**
740 **as a function of the irrigation treatment.**

	Grapefruit (t_2)		Mandarin (t_2)	
Treatment	Ψ_π	Ψ_P	Ψ_π	Ψ_P
TW-C	-1.55±0.08b	0.65±0.10	-1.73±0.03b	0.83±0.04a
TW-RDI	-1.72±0.08a	0.75±0.09	-1.64±0.08b	0.79±0.03a
RW-C	-1.70±0.06a	0.80±0.11	-1.85±0.05a	1.06±0.04b
RW-RDI	-1.69±0.09a	0.68±0.08	-1.80±0.01a	1.04±0.05b
Significance	*	ns	*	*

741 **Each value is the average ± SE of eight replicates. Different letters in the column indicate significant differences among**
742 **treatments according to Duncan's test (P <0.05). ns: not significant; t_2: 10.00 GMT; Ψ_π: osmotic potential; Ψ_P: pressure**
743 **potential.**

744

745

Table 4. Gas-exchange parameters in Citrus species as a function of the irrigation treatment.

	Grapefruit				Mandarin			
	t_1		t_2		t_1		t_2	
Treatment	A	g_s	A	g_s	A	g_s	A	g_s
TW-C	14.16±0.95b	193.36±2.53c	10.68±0.04b	117.54±0.22c	6.37±0.16	50.04±0.04b	3.40±0.34b	30.09±0.03b
TW-RDI	12.87±0.54a	138.11±6.64b	7.26±0.01a	91.73±0.01b	7.00±0.35	50.48±0.06b	1.50±0.12a	20.12±0.04a
RW-C	12.21±0.10a	113.81±1.13a	8.46±0.58a	98.12±5.88b	6.07±0.79	40.01±0.03a	3.10±0.04b	30.09±0.02b
RW-RDI	13.06±1.04a	120.76±5.45a	7.36±0.65a	70.50±8.63a	7.10±1.46	50.5±0.10b	2.52±0.59b	25.00±0.54b
Significance	*	*	*	*	ns	*	*	*

Each value is the average ± SE of eight replicates. Different letters in the column indicate significant differences among treatments according to Duncan's test (P <0.05). A: Net photosynthesis (μmol·m^{-2}·s^{-1}); g_s: stomatal conductance (mmol·m^{-2}·s^{-1}); ns: not significant; RW-C: reclaimed water-control; RW-RDI: reclaimed water-regulated deficit irrigation; TW-C: transfer water-control; TW-RDI: transfer water-regulated deficit irrigation; t_1: 07.00 GMT; t_2: 10.00 GMT.

Table 5. Leaf structural traits in Citrus species as a function of the irrigation treatment.

	Grapefruit				Mandarin			
Treatment	LMA	Cl^-	B	Na	LMA	Cl^-	B	Na
TW-C	143.37±1.39b	0.42±0.04a	83.25±5.60a	0.02±0.00a	110.91±1.93a	0.48±0.08a	75.70±5.04a	0.02±0.00a
TW-RDI	146.96±1.37b	0.36±0.04a	87.00±7.44a	0.02±0.00a	111.50±4.35a	0.46±0.06a	75.99±0.96a	0.03±0.01a
RW-C	122.82±2.80a	0.58±0.06b	105.26±1.36b	0.07±0.01b	111.46±1.52a	0.76±0.09b	92.60±8.41ab	0.08±0.00b
RW-RDI	127.00±2.49a	0.54±0.05ab	112.96±9.08b	0.08±0.01b	120.72±1.15b	0.56±0.04a	115.09±1.77b	0.05±0.01ab
Significance	*	*	*	*	*	*	*	*

Values represent average ± SE of eight replicates. Different letters in the column indicate significant differences among treatments according to Duncan's test (P <0.05).

B: boron (mg·kg-1); Cl^-: chloride ion (%); LMA: Leaf dry mass per unit area ($g \cdot m^{-2}$); Na: sodium (%); RW-C: reclaimed water-control; RW-RDI: reclaimed water-regulated deficit irrigation; TW-C: transfer water-control; TW-RDI: transfer water-regulated deficit irrigation.

Table 6. Spectral indicators in Citrus species as a function of the irrigation treatment.

		t_1			t_2		
	Treatment	**R**	**NIR**	**NDVI**	**R**	**NIR**	**NDVI**
Grapefruit	**TW-C**	69.51±2.33a	171.73±2.5	0.4116±0.0056b	65.81±1.80a	149.13±1.1b	0.4047±0.0085
	TW-RDI	77.20±1.35b	162.65±3.4	0.4165±0.0102b	65.84±1.99a	144.91±1.3a	0.3905±0.0121
	RW-C	80.11±2.49b	166.48±4.1	0.3982±0.0087a	71.18±2.08b	150.0±1.0b	0.3936±0.0046
	RW-RDI	85.10±2.41b	169.83±1.8	0.3984±0.0024a	69.37±1.02b	142.60±1.9a	0.3975±0.0153
	Significance	*	ns	*	*	*	ns
		t_1			t_2		
	Treatment	**R**	**NIR**	**NDVI**	**R**	**NIR**	**NDVI**
Mandarin	**TW-C**	71.77±0.69a	160.21±4.06a	0.4164±0.0034b	64.96±2.89a	150.73±5.73	0.4166±0.0118
	TW-RDI	71.52±1.06a	177.35±1.39b	0.3837±0.0067a	70.12±1.27b	153.79±3.80	0.4052±0.0089
	RW-C	75.89±2.00b	165.70±1.18a	0.4048±0.0016b	64.42±1.08a	149.43±2.04	0.4276±0.0102
	RW-RDI	83.14±1.22c	176.19±0.95b	0.3934±0.0027a	65.57±2.15a	146.27±3.70	0.4090±0.0162
	Significance	*	*	*	*	ns	ns

Each value is the average ± SE of eight replicates. Different letters in the column indicate significant differences among treatments according to Duncan's test (P <0.05).

NDVI: normalized difference vegetation index (dimensionless); NIR: near-infrared (digital number); ns: not significant; R: Red (digital number); RW-C: reclaimed water-control; RW-RDI: reclaimed water-regulated deficit irrigation; TW-C: transfer water-control; TW-RDI: transfer water-regulated deficit irrigation; t_1: 07.00 GMT; t_2: 10.00 GMT.

766

Table 7. Relationships between plant water status and leaf structural traits with spectral indicators in Citrus species.

Grapefruit																
A)	**Ψ_s**		**Ψ_π**		**Ψ_P**		**A**		**g_s**		**Chl T**		**Coef a/b**		**LMA**	
	s	**R^2**	**s**	**R^2**	**s**	**R^2**	**s**	**R^2**	**s**	**R^2**	**s**	**R^2**	**s**	**R^2**	**s**	**R^2**
R	+	0.34	-	0.18	+	0.62***	+	0.33	+	0.02	-	0.50**	+	0.39*	-	0.22
NIR	+	0.54*	+	0.04	+	0.17	+	0.89***	+	0.61**	+	0.05	-	0.00	-	0.04
NDVI	-	0.00	+	0.17	-	0.09	+	0.53*	+	0.55*	+	0.19	-	0.21	+	0.26
Mandarin																
B)	**Ψ_s**		**Ψ_π**		**Ψ_P**		**A**		**g_s**		**Chl T**		**Coef a/b**		**LMA**	
	s	**R^2**	**s**	**R^2**	**s**	**R^2**	**s**	**R^2**	**s**	**R^2**	**s**	**R^2**	**s**	**R^2**	**s**	**R^2**
R	+	0.42*	-	0.00	+	0.07	+	0.51*	+	0.44*	-	0.07	-	0.06	+	0.12
NIR	+	0.78***	+	0.04	+	0.02	+	0.77***	+	0.71***	-	0.01	-	0.10	+	0.30
NDVI	-	0.71***	-	0.21	-	0.00	-	0.30	-	0.24	+	0.02	+	0.00	-	0.08

Significance level: * p<0.05;p<0.01; ***p<0.005.**

Shaded boxes correspond to significant relationships according to Pearson correlation coefficients.

Regression lines were calculated with eight points corresponding to the mean values of each treatment at t_1 and t_2.

A: net gas exchange ($\mu mol \cdot m^{-2} \cdot s^{-1}$); Chl T: leaf total chlorophyll ($mg \cdot g_{FM}^{-1}$); Coef a/b: coefficient Chl a/Chl b; g_s: stomatal conductance ($mmol \cdot m^{-2} \cdot s^{-1}$); LMA: leaf dry mass per unit area ($g \cdot m^{-2}$); NDVI: normalized difference vegetation index; NIR: near-infrared; R^2: coefficients of determination; s: slope sign; Ψ_P: pressure potential (MPa); Ψ_s: stem water potential (MPa); Ψ_π: osmotic potential (MPa); R: Red .

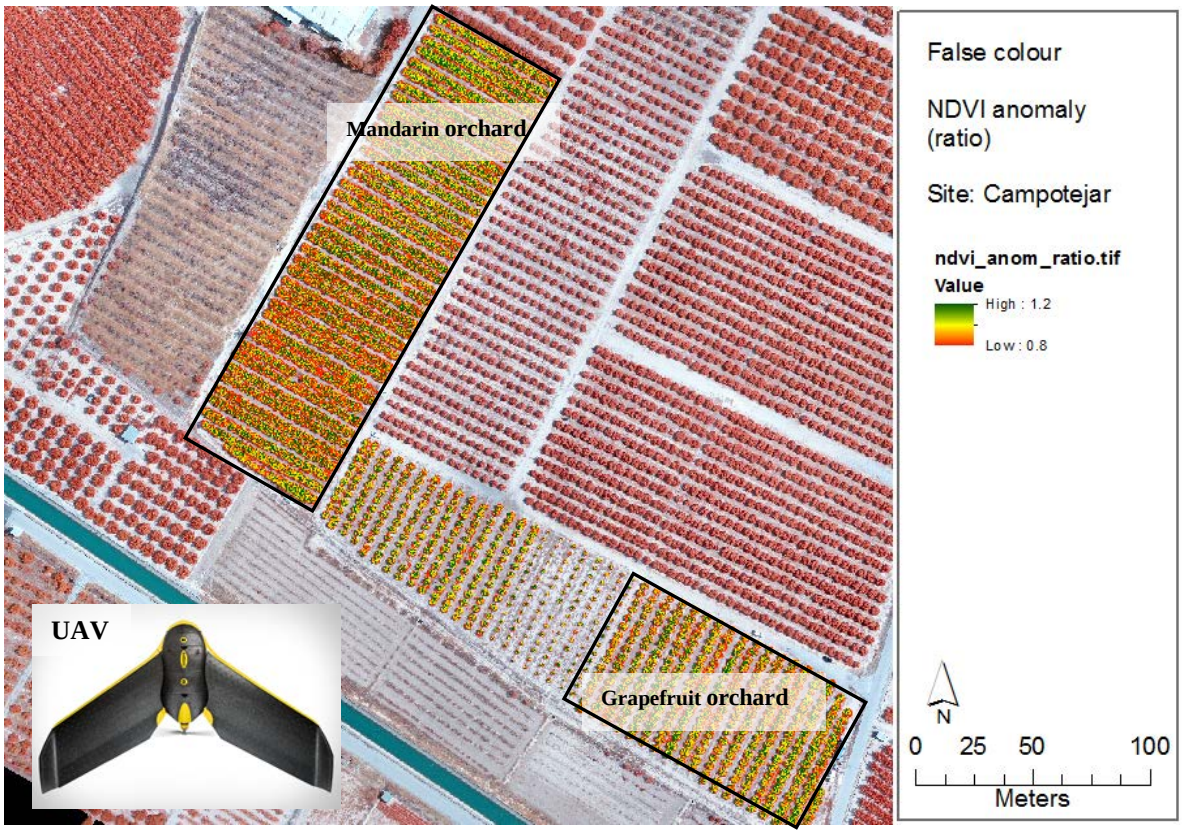

Figure 1. Citrus orchards and fixed-wing unmanned aerial vehicle (eBee SenseFly) used in the current study.

NDVI: normalized difference vegetation index; UAV: unmanned aerial vehicle.

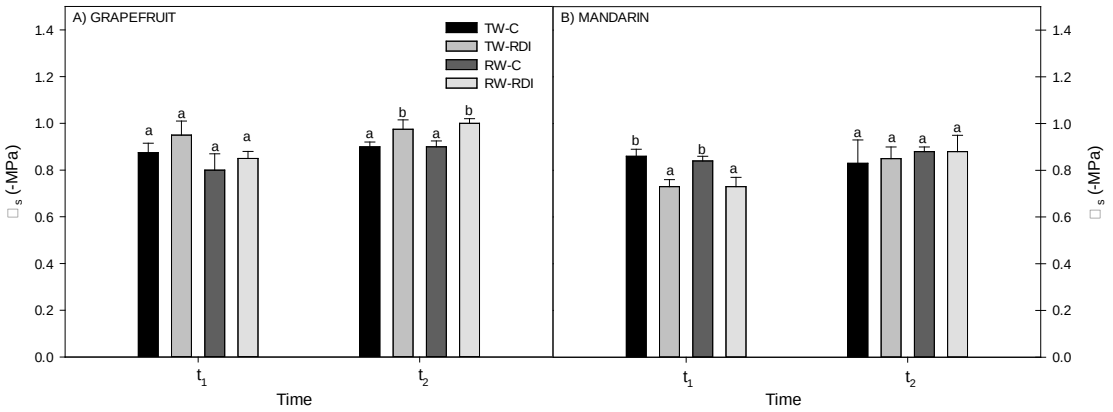

Figure 2. Stem water potential in Citrus species.

Each value is the average ± SE of eight replicates. Different letters on the bars indicate significant differences according to Duncan's test ($P<0.05$) for the treatments within t_1 or t_2. RW-C: reclaimed water-control; RW-RDI: reclaimed water-regulated deficit irrigation; TW-C: transfer water-control; TW-RDI: transfer water-regulated deficit irrigation; t_1: 07.00 GMT; t_2: 10.00 GMT; Ψ_s: stem water potential (MPa).

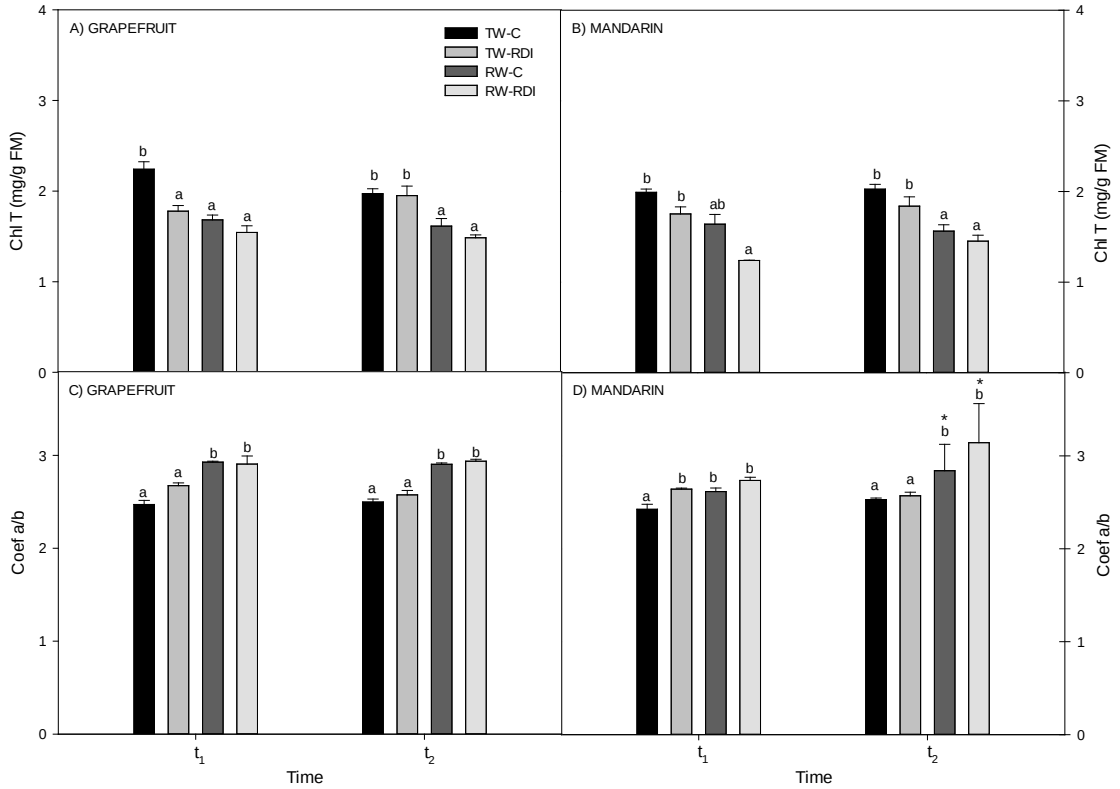

Figure 3. Total leaf chlorophyll and coefficient Chl a/Chl b for grapefruit (A and C, respectively) and mandarin (B and D, respectively) trees as a function of the irrigation treatment.

Each value is the average ± SE of eight replicates. Different letters on the bars indicate significant differences among treatments according to Duncan's test ($P<0.05$) at t_1 or t_2. *corresponds to significant differences by ANOVA test between t_1 and t_2 within the same treatment in mandarin. Chl T: total leaf chlorophyll ($mg \cdot g_{FM}^{-1}$); Coef a/b: coefficient Chl a/Chl b; RW-C: reclaimed water-control; RW-RDI: reclaimed water-regulated deficit irrigation; TW-C: transfer water-control; TW-RDI: transfer water-regulated deficit irrigation; t_1: 07.00 GMT; t_2: 10.00 GMT.

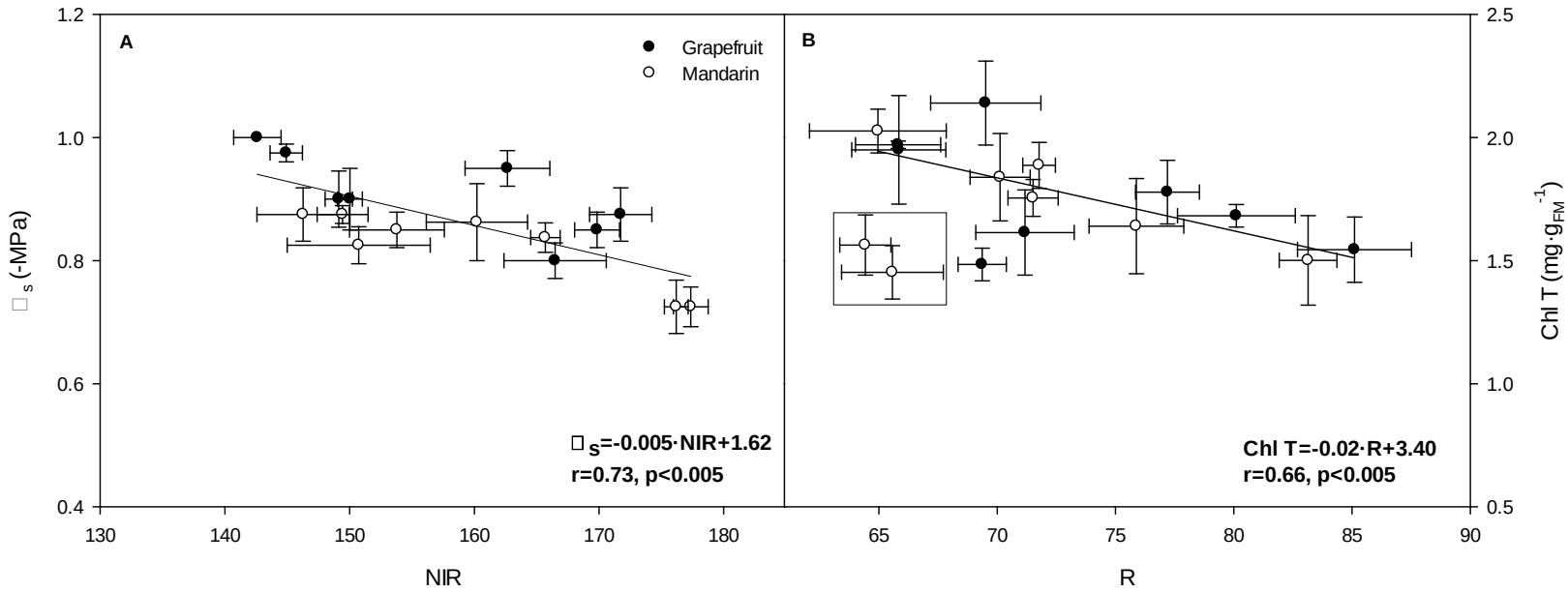

Figure 4. Correlations between A) Near infrared and water potential (Ψ_s, -MPa); B) Red (R) domain and Chlorophyll Total (Chl T, mg·g_{FM}^{-1}) for both species together.

Regression lines were calculated with 16 points corresponding to the mean values of each treatment at t_1 and t_2 and both species. Points surrounded by a square correspond to RW treatments of mandarin at t_2. Chl T: total leaf chlorophyll (mg·g_{FM}^{-1}); NIR: near infrared; R: red; t_1: 07.00 GMT; t_2: 10.00 GMT; Ψ_s: stem water potential (MPa).